A decision-making Fokker-Planck model in computational neuroscience

José Antonio Carrillo, Stéphane Cordier, Simona Mancini

Journal of Mathematical Biology manuscript No.
(will be inserted by the editor)

A Decision-Making Fokker-Planck Model in Computational Neuroscience

José Antonio Carrillo · Stéphane Cordier · Simona Mancini

Received: date / Accepted: date

Abstract In computational neuroscience, decision-making may be explained analyzing models based on the evolution of the average firing rates of two interacting neuron populations, e.g. in bistable visual perception problems. These models typically lead to a multi-stable scenario for the concerned dynamical systems. Nevertheless, noise is an important feature of the model taking into account both the finite-size effects and the decision's robustness. These stochastic dynamical systems can be analyzed by studying carefully their associated Fokker-Planck partial differential equation. In particular, in the Fokker-Planck setting, we analytically discuss the asymptotic behavior for large times towards a unique probability distribution, and we propose a numerical scheme capturing this convergence. These simulations are used to validate deterministic moment methods recently applied to the stochastic differential system. Further, proving the existence, positivity and uniqueness of the probability density solution for the stationary equation, as well as for the time evolving problem, we show that this stabilization does happen. Finally, we discuss the convergence of the solution for large times to the stationary state. Our approach leads to a more detailed analytical and numerical study of decision-making models applied in computational neuroscience.

Keywords Computational Neuroscience · Fokker-Planck Equation · General Relative Entropy

J.A. Carrillo
ICREA (Institució Catalana de Recerca i Estudis Avançats)
and Departament de Matemàtiques
Universitat Autònoma de Barcelona, E-08193 Bellaterra, Spain
Tel.: +34-93-5814548
E-mail: carrillo@mat.uab.es

S. Cordier, S. Mancini
Fédération Denis Poisson (FR 2964)
BP. 6759, Department of Mathematics (MAPMO UMR 6628)
University of Orléans and CNRS, F-45067 Orléans, France

1 Introduction

The derivation of biologically relevant models for the decision-making processes done by animals and humans is an important question in neurophysiology and psychology. The choice between alternative behaviours based on perceptual information is a typical example of a decision process. It is quite common to observe bi-stability in several psychological experiments widely used by neuroscientists. Archetypical examples of these multi-stable decision-making processes are bistable visual perception, that is, two distinct possible interpretations of the same unchanged physical retinal image: Necker cube, Rubins face-vase, binocular rivalry and bistable apparent motion [6,12,20].

In order to explain these phenomena, biologically realistic noise-driven neural circuits have been proposed in the literature [9] and even used to qualitatively account for some experimental data [23]. The simplest model consists of two interacting families of neurons, each one characterized by its averaged firing rate (averaged number of spikes produced per time). Correlation of these neuron families is bigger with their own behavior than with the others. Moreover, this mechanism is mediated by inhibition from the rest of the neurons and the sensory input. The external stimuli may produce an increasing activity of one of the neuron families leading to a decision state in which we have a high/low activity ratio of the firing rates. Decision-making in these models is then understood as the fluctuation-driven transition from a spontaneous state (similar firing rates of both families) to a decision state (high/low activity level ratio between the two families).

As has already been explained and discussed in different works [11,12,22], the theory of stochastic dynamical systems offers a useful framework for the investigation of the neural computation involved in these cognitive processes. Noise is an important ingredient in these models. In fact, such neural families are comprised of a large number of spiking neurons, so that fluctuations arise naturally through noisy input and/or disorder in the collective behaviour of the network. Moreover, this is used to introduce a finite-size effect of the neuron families as discussed in [11,12].

Many other works can be found in the recent literature concerning decision-making stochastic differential models and the understanding of the evaluation of a decision, see for instance [8] for a review paper, or [16] for a review on the different ways to compute a decision at different biological levels. Moreover, we refer to [10,15,24,27] for results concerning two choices task paradigm. On the one hand, all these models give good approximations of the reaction times (RT), but on the other hand, most of them consider linear or linearized stochastic differential systems. Thus, it is possible to give explicitly their reduction to a one-dimensional drift-diffusion (or Fokker-Planck) equation, and hence they can be explicitly solved as in the case of the Ornstein-Uhlenbeck process.

The stochastic differential system we shall consider in the sequel is nonlinear, and the progressive Kolmogorov equation (or the Fokker-Planck) describing the probability density function, in the two dimensional parameter

space, is characterized by a drift term not being the gradient of a potential. The closest example in the literature to our approach is the numerical treatment reported in [10, Section 3.3] for a nonlinear stochastic differential system. As mentioned in [10], no explicit information is thus available on the behavior of the solution, and no explicit reduction to a one-dimensional problem is possible, as will be further discussed in Section 4.

Therefore, in this paper we want to focus on showing that for this class of nonlinear stochastic dynamical systems, one can exhibit large time stabilization at the level of the probability distribution given by its associated Fokker-Planck equation. This fact is not at all obvious from the stochastic dynamical system and it is the main improvement with respect to the studies in [11,10]. The analysis of the trend towards this stationary state is biologically relevant. In particular, we can compute the probability of reaching a particular decision by integrating the stationary distribution function in a suitable region around the particular decision state. Moreover, one can compute important information for the decision making problem such as reaction times, i.e., the average time to reach a decision. This question can be related with the rate of convergence towards equilibrium.

We will analyze this stabilization issue by numerical and analytical methods. We start by performing numerical simulations on the Fokker-Planck model showing the large time behavior of the probability density. Moreover, we validate the results obtained by [11] using a deterministic moment method for the associated stochastic differential system. Finally, we will prove the existence and uniqueness of the stationary probability distribution and its asymptotic stability, that is, the convergence of the time dependent probability density to the unique solution of the stationary problem.

The precise model considered in this work uses a Wilson-Cowan [25] type system, describing the time evolution of two population of neurons firing rates ν_i, $i = 1, 2$:

$$\tau \frac{d\nu_i(t)}{dt} = -\nu_i(t) + \phi\left(\lambda_i + \sum_{j=1,2} w_{ij}\nu_j(t)\right) + \xi_i(t), \quad i = 1, 2, \tag{1}$$

where τ is the typical time relaxation and $\xi_i(t)$, $i = 1, 2$, represent a white noise of amplitude β, i.e., they correspond to independent brownian motions with the same variance $\beta^2/2$.

In (1) the function $\phi(x)$ has a sigmoidal shape determining the response function of the neuron population to a mean excitation x given by $x_i(t) = \lambda_i + \sum_j w_{ij}\nu_j$, $i = 1, 2$, in each population:

$$\phi(x) = \frac{\nu_c}{1 + \exp(-\alpha(x/\nu_c - 1))}, \tag{2}$$

where λ_i are the external stimuli applied to each neuron population and w_{ij} are the connection coefficients. The parameter ν_c represents both the maximal activity rate of the population and the frequency input needed to drive the population to half of its maximal activity.

Following [21,17,11], we assume that neurons within a specific population are likely to correlate their activity, and to interact via strong recurrent excitation with a dimensionless weight $w_+ > 1$ greater than a reference baseline value established to 1. Analogously, neurons in two different populations are likely to have anti-correlated activity expressed by a excitatory weight lower than baseline, $w_- < 1$. Furthermore, we assume that there is global feedback inhibition, as a result of which all neurons are mutually coupled to all other neurons in an inhibitory fashion (we will denote this inhibitory weight by w_I). As a result, the synaptic connection coefficients w_{ij}, representing the interaction between population i and j, are the elements of a 2×2 symmetric matrix W given by

$$W = \begin{bmatrix} w_+ - w_I & w_- - w_I \\ w_- - w_I & w_+ - w_I \end{bmatrix},$$

The typical synaptic values considered in these works are such that $w_- < w_I < w_+$ leading to cross-inhibition and self-excitation.

Applying standard methods of Ito calculus, see for instance [14], we can prove that the probability density $p = p(t, \nu)$ of finding the neurons of both populations firing at averaged rates $\nu = (\nu_1, \nu_2)$ at $t > 0$, satisfies a Fokker-Planck equation, also known as the forward Kolmogorov equation. Hence, $p(t, \nu)$ must satisfy:

$$\partial_t p + \nabla \cdot \left(\left[-\nu + \Phi(\Lambda + W \cdot \nu) \right] p \right) - \frac{\beta^2}{2} \Delta p = 0 \tag{3}$$

where $\nu \in \Omega = [0, \nu_m] \times [0, \nu_m]$, $\Lambda = (\lambda_1, \lambda_2)$, $\Phi(x_1, x_2) = (\phi(x_1), \phi(x_2))$, $\nabla = (\partial_{\nu_1}, \partial_{\nu_2})$ and $\Delta = \Delta_\nu$. We choose to complete equation (3) by the following no-flux boundary conditions:

$$\left(\left[-\nu + \Phi(\Lambda + W \cdot \nu) \right] p - \frac{\beta^2}{2} \nabla p \right) \cdot n = 0 \tag{4}$$

where n is the outward normal to the domain Ω. Physically, these boundary conditions mean that neurons cannot spike with arbitrarily large firing rates and thus there is a typical maximal value of the averaged firing rate ν_m and that the solution to (3) is a probability density function, i.e.,

$$\int_\Omega p(t, \nu) \, d\nu = 1. \tag{5}$$

In order to simplify notations, we will from now on consider the vector field $F = (F_1, F_2)$, representing the flux in the Fokker-Planck equation:

$$F = -\nu + \Phi(\Lambda + W \cdot \nu) = \begin{pmatrix} -\nu_1 + \phi(\lambda_1 + w_{11}\nu_1 + w_{12}\nu_2) \\ -\nu_2 + \phi(\lambda_2 + w_{21}\nu_1 + w_{22}\nu_2) \end{pmatrix} \tag{6}$$

then, equation (3) and boundary conditions (4) read:

$$\partial_t p + \nabla \cdot \left(F \, p - \frac{\beta^2}{2} \nabla p \right) = 0 \tag{7}$$

$$\left(F\,p - \frac{\beta^2}{2}\nabla p\right)\cdot n = 0 \tag{8}$$

In the absence of noise, the deterministic dynamical system corresponding to (1) has a region of parameters exhibiting a multi-stable regime. In this multi-stable framework, the relevant fixed-point solutions are the spontaneous and the two decision states. Spontaneous state corresponds to the case in which no decision is taken and without impulse neurons remains in this state, see [12]. In particular, in the bistable case, the spontaneous state is unstable, and only the two decision states are stable. For sufficiently strong inhibition w_I the two decision states are bistable with respect to one another. Indeed, the deterministic dynamical system is not a gradient flow.

Section 2 is devoted to the numerical study of the model above, and to the discussion of the numerical results and their relation with those of [22,11,12]. The only direct study of the Fokker-Planck approach that we are aware of has been performed in [10]. It shows by direct finite element discretisation that the evolution of a Fokker-Planck equation up to a fixed time can be useful for computing reaction times. Still, the trend to equilibrium for large times is neither shown nor analyzed.

Moreover, although the mathematical problem corresponding to (7)-(8) is linear, it has not been dealt with in detail due to its non classical boundary conditions. Despite the linearity of (7) in p, we cannot have an explicit solution in exponential form to the associate steady state problem. Indeed, the drift vector F is not the gradient of a potential V, as it can be easily checked. Hence, it is not possible to give an explicit expression of the type $\exp(-2V/\beta^2)$ as for the Ornstein-Uhlenbeck process, of the steady states of equation (7). Nevertheless, in Sect. 3.3 we will show that the steady state solution has an exponential shape. This question is related to general problems of Fokker-Planck equations with non-gradients drifts [2,3] arising also in polymer fluid flow problems [4].

In fact, in a bounded domain Ω and under the assumption that the flux F is regular enough and incoming in the domain $F\cdot n < 0$, we will show the existence of an unique positive normalized steady state p_∞, or equilibrium profile, for the problem (7)-(8). This assumption on the drift F is verified in our particular computational neuroscience model for ν_m large enough. In order to obtain this theorem, we use classical functional analysis theorems via a variant of the Krein-Rutman theorem. This will be the first objective of Section 3. We will also prove existence, uniqueness and positivity of the probability density solution of the evolutionary Fokker-Planck equation, and its convergence towards the unique normalized steady state. This result shows the global asymptotic stability of this unique stationary state leading to the final probability of the decision states in our neuroscience model. Rate of convergence is an open problem directly related with estimating the spectral gap. The estimation of the first positive eigenvalue for the Fokker-Planck equation is directly linked to the reaction time estimation.

2 Numerical Discretization and Large time Equilibrium

In this section, we will consider a particular relevant case of the neuroscience model discussed in the introduction, exactly corresponding to the discussion in [11]. We will consider the following values of the synaptic connection parameters: $w_+ = 2.35$, $w_I = 1.9$ and $w_- = 1 - r(w_+ - 1)/(1 - r)$, $r = 0.3$, (which correspond to self-excitation and cross-inhibition between the two neuron families). The sigmoidal response function is determined from $\alpha = 4$ and $\nu_c = 20Hz$ with external stimuli corresponding to two cases: $\lambda_1 = 15Hz$ and $\lambda_2 = \lambda_1 + \Delta\lambda$, with $\Delta\lambda = 0$ for the unbiased case or $\Delta\lambda = 0.1$ for the biased one; i.e. when one of the two decision states is highlighted with respect to the other. In the unbiased case, the situation is completely symmetric, and so is the solution. However, in the biased case only one of the two decision states will be reached with large probability. The relaxation time for the system is chosen to $\tau = 10^{-2}s$.

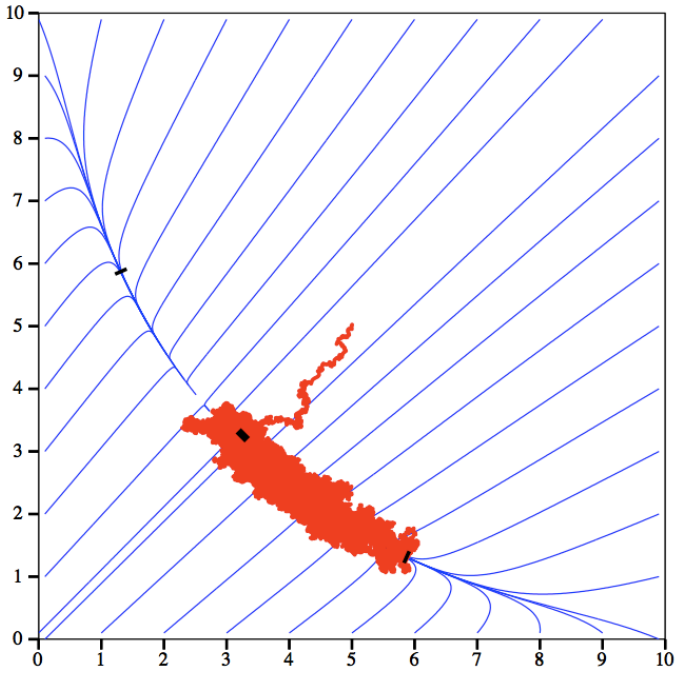

Fig. 1 Dynamics in the unbiased case of (1) in the deterministic system (straight lines) and the stochastic system (wiggled line). Straight lines emphasize the location of the equilibrium points over the slow-manifold of the system. The black bars are the equilibrium points of the differential system (denote by S_i with $i = 1, 2, 3$ in the sequel). The particle starts its dynamics in point $(5, 5)$, moves almost straight forward towards the slow-manifold, and then slowly oscillates towards one of the stable points/decision states.

By means of direct simulations of the stochastic differential system (1), it can be shown that there is a *slow-fast* behavior of the solutions towards equilibrium. More precisely, it is possible to show that system (1) is characterized by two stable and one unstable equilibrium points, see [11]. For example, in the unbiased case, if $\Delta\lambda = 0$, the stable decision states are in $S_1 = (1.32, 5.97)$ and its symmetric $S_3 = (5.97, 1.32)$, and the unstable spontaneous state is in $S_2 = (3.19, 3.19)$. In contrast with this, in the biased case $\Delta\lambda = 0.1$ the stable decision states are in $S_1 = (1.09, 6.59)$ and $S_3 = (5.57, 1.53)$ and the unstable spontaneous state is in $S_2 = (3.49, 3.08)$. Thus, in figure 1 we highlight, in the unbiased case, the fast convergence of one realization of (1) towards the slow-manifold to which the equilibrium points belong, and its very slow convergence towards one of the two stable points. The discussion of this behaviour is beyond the goal of this paper, and a possible way to use the slow-fast feature of the differential system (1) will be investigated in future work.

We will now propose a numerical scheme to approximate the solution of the Fokker-Planck equation (7). Let us first comment that a direct approximation by simple finite differences has an important drawback in terms of computing time. The main issue being this slow-fast feature of the system, producing then a kind of metastable solution that takes a long time to evolve to the final equilibrium solution concentrating its probability around the decision states.

In order to discretise and perform numerical simulations of equation (7), we apply an explicit finite volume method on the bounded domain $\Omega = [0, \nu_m] \times [0, \nu_m]$. In the following numerical simulations we choose ν_m=10, which is large enough in order to verify the incoming flux condition: $F \cdot n < 0$. In order to simplify notations below, we have set $\tau = 1$, but in the figures the time scale has been adjusted to take into account the relaxation time τ in order to render our results comparable to those in [11] discussed below.

Let $i = 0...M_1 - 1$ and $j = 0...M_2 - 1$, and consider the discrete variables:

$$n_i = \nu_1(i) = \left(i + \frac{1}{2}\right) \Delta\nu_1,$$

$$n_j = \nu_2(j) = \left(j + \frac{1}{2}\right) \Delta\nu_2,$$

where $\Delta\nu_1$ and $\Delta\nu_2$ are the mesh size along the ν_1 and ν_2 direction respectively:

$$\Delta\nu_i = \frac{\nu_m}{M_i}.$$

Thus, the discrete variables n_i are defined at the centre of the squared cells. Moreover, let Δt be the time discretisation step, so that $p^k(i, j)$ represents the distribution function $p(k\Delta t, n_i, n_j)$. We note that $p^k(i, j)$ are the unknown values of the discretized distribution function inside the meshes, whereas $p^k(i - \frac{1}{2}, j - \frac{1}{2})$ are the interpolated values at their interfaces. The discretized Fokker-Planck equation is then given by:

$$p^{k+1}(i, j) = p^k(i, j) + \Delta t \mathcal{F}^k(i, j), \tag{9}$$

where :

$$\mathcal{F}^k(i,j) = \frac{1}{\Delta\nu_1}\left(F^k\left(i+\frac{1}{2},j\right) - F^k\left(i-\frac{1}{2},j\right)\right) + \frac{1}{\Delta\nu_2}\left(G^k\left(i,j+\frac{1}{2}\right) - G^k\left(i,j-\frac{1}{2}\right)\right),$$

with $F^k(i+\frac{1}{2},j)$ and $G^k(i,j+\frac{1}{2})$ the fluxes at the interfaces respectively defined by :

$$F^k\left(i+\frac{1}{2},j\right) = \left(-n_{i+1/2} + \phi(\lambda_1 + w_{11}n_{i+1/2} + w_{12}n_j)\right)p^k\left(i+\frac{1}{2},j\right) - \frac{\beta^2}{2\Delta\nu_1}\left(p^k(i+1,j) - p^k(i,j)\right),$$

$$G^k\left(i,j+\frac{1}{2}\right) = \left(-n_{j+1/2} + \phi(\lambda_2 + w_{21}n_i + w_{22}n_{j+1/2})\right)p^k\left(i,j+\frac{1}{2}\right) - \frac{\beta^2}{2\Delta\nu_2}\left(p^k(i,j+1) - p^k(i,j)\right).$$

We choose the most simple interpolation at the interfaces:

$$p^k\left(i+\frac{1}{2},j\right) = \frac{p^k(i+1,j) + p^k(i,j)}{2},$$

and

$$p^k\left(i,j+\frac{1}{2}\right) = \frac{p^k(i,j+1) + p^k(i,j)}{2}.$$

Remark 1 Concerning the CFL condition and in order to diminish the computational time, we compute an adaptive time step Δt at every iteration. We require, for example, that:

$$\frac{p^k(i,j)}{2} \leq p^{k+1}(i,j) \leq \frac{3p^k(i,j)}{2}.$$

These conditions lead to the following time step bound:

$$\Delta t|\mathcal{F}^k(i,j)| \leq \frac{p^k(i,j)}{2}.$$

Finally we define at each iteration the following Δt, for i,j such that $p^k(i,j) \neq 0$ and $\mathcal{F}^k(i,j) \neq 0$:

$$\Delta t = \min_{i,j} \frac{p^k(i,j)}{2|\mathcal{F}^k(i,j)|}.$$

This adaptive time step condition gains a factor 100 in the time computations with respect to the classical one, but it depends on the number of discretisation points. For instance, in our simulations we need at least $M_1 = M_2 = 200$ in order to capture the growth of the double picked distribution.

Finally, we choose to stop our computation when the difference between two successive distribution profiles is smaller than 10^{-10}, and we say in this case that we have reached the equilibrium.

Using the above discretisation we compute various quantities as the marginals $N_1(t,\nu_1)$ and $N_2(t,\nu_2)$ of the distribution function p:

$$N_1(t,\nu_1) = \int_0^{\nu_m} p(\nu_1,\nu_2,t)d\nu_2,$$

$$N_2(t,\nu_2) = \int_0^{\nu_m} p(\nu_1,\nu_2,t)d\nu_1,$$

representing the behaviour of each neuron population. We compute as well the first $\mu_1(t),\mu_2(t)$ and second $\gamma_{11}(t),\gamma_{12}(t),\gamma_{22}(t)$ moments associated to the distribution function p. They are respectively given by:

$$\mu_i(t) = \int_\Omega \nu_i p(\nu_1,\nu_2,t)d\nu_1 d\nu_2, \quad i=1,2,$$

$$\gamma_{ij}(t) = \int_\Omega \nu_i\nu_j p(\nu_1,\nu_2,t)d\nu_1 d\nu_2, \quad i,j=1,2.$$

Moreover, we can compute the probabilities $\rho_i(t)$ for a couple of firing rates (ν_1,ν_2) to belong to some domains Ω_i:

$$\rho_i(t) = \int_{\Omega_i} p(\nu_1,\nu_2,t)d\nu_1 d\nu_2.$$

In particular, the domains Ω_i will be three boxes centered at the three equilibrium points: $\Omega_1 = [0,2]\times[5,10]$ and $\Omega_3 = [5,10]\times[0,2]$ for the two stable points S_1 and S_3, $\Omega_2 = [2,5]\times[2,5]$ for the unstable one, S_2. In fact, $\rho_i(t)$ represents the probability in time of reaching the decision state S_i for $i=1$ and $i=3$, while $\rho_2(t)$ gives information about the probability in time to leave the spontaneous state.

We present now some numerical results, obtained starting from an initial condition given by a Gaussian centered at $(3,3)$, near the unstable position S_2, as in [11]. We considered here both the unbiased ($\Delta\lambda = 0$) and the biased ($\Delta\lambda = 0.1$) case, both with a standard deviation $\beta = 0.1$.

In figure 2 we represent the evolution in time of the marginal $N_1(t)$. In the unbiased case (left), it is clearly shown the convergence of the density probability function towards an equilibrium with a double pick distribution. Moreover, we remark the slow-fast behaviour of the distribution when evolving in time: fast diffusion, and slow growth of the two picks. In the biased case (right), the distribution function at equilibrium is mostly concentrated around one of the two decision points. The bias is strong enough to make converge the firing rates, almost instantaneously, to only one of the two decision states.

In figure 3 we show the contour levels of the density $p_\infty(\nu_1,\nu_2)$ at equilibrium in the unbiased case (left) and the biased case (right). We note that there are two points of mass concentration around S_1 and S_3 which are the

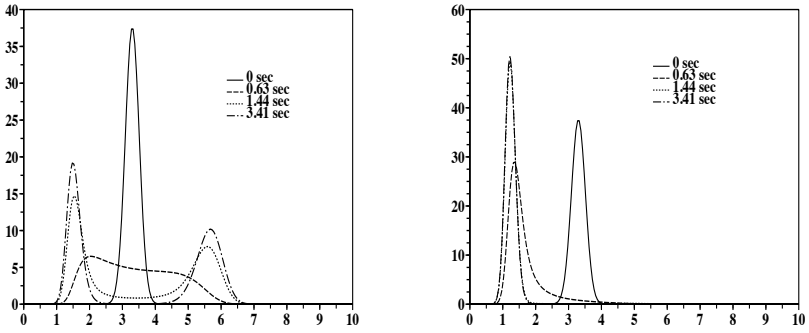

Fig. 2 Time evolution for the marginals $N_1(t, \nu_1)$. Left: unbiased case. Right: biased case; the curve for 1.44 sec and the final one at 3.41 seconds overlaps since we have almost reached the equilibrium profile.

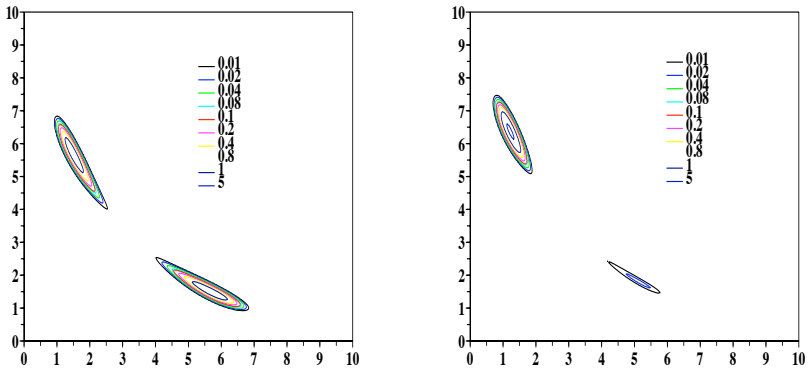

Fig. 3 Contour level for the equilibrium solution. Left: unbiased case. Right: biased case.

stable equilibrium points of system (1). We remark that, in the unbiased case the probability density is symmetrically distributed along the slow-manifold. In contrast with this, in the biased case there is no symmetry: almost a zero proportion of the population is still concentrated around one of the stable points, namely S_3. This is due to the slow behavior of the system, and one should wait for a very long time in order to have all the population of neurons centered around the S_1 decision state.

In figure 4 we show, only for the unbiased case, the evolution in time of the moments of order one, μ_1 and μ_2 (on the left), and two, γ_{11}, γ_{12} and γ_{22} (on the right).

This computation recovers in a exact manner the approximation on the evolution of moments done in [11]. The moment method has been used in the computational neuroscience community [22,11,12] in order to approximate

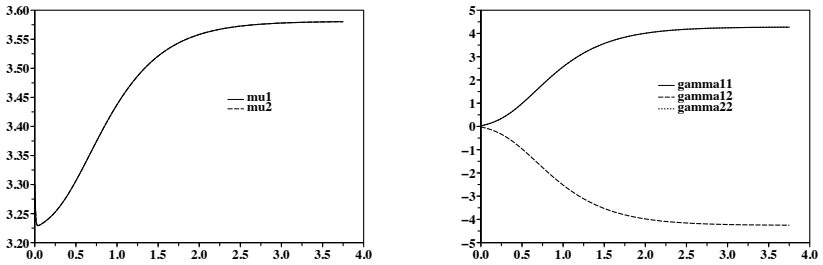

Fig. 4 Moments $\mu_1, \mu_2, \gamma_{11}, \gamma_{12}, \gamma_{22}$ with respect to time, in the unbiased case.

the collective averaged quantities of the stochastic differential system (1) by solving deterministic systems.

These moment methods need a closure assumption in order to give closed systems of equations and, therefore, they have inherent errors in their approximation. Nevertheless, in this particular case they lead to good qualitative approximations comparing our results to the ones in [11], whose detailed numerical study is currently under way.

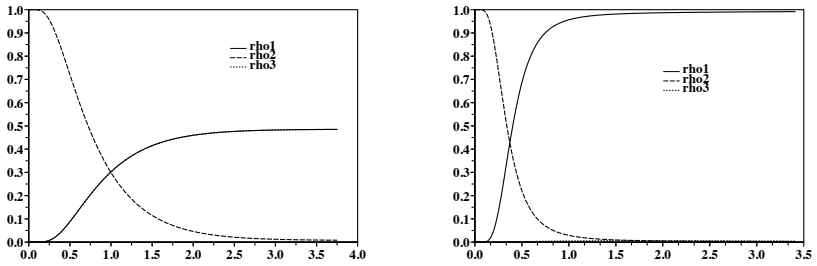

Fig. 5 Evolution in time of the densities $\rho_i(t)$. Left: unbiased case; we note that ρ_1 and ρ_3 perfectly overlap. Right: biased case.

In figure 5 we show the evolution in time of three probabilities, ρ_i for $i = 1, 2, 3$, of finding the firing rates in three different domains $\Omega_1 = [0, 2] \times [5, 10]$, $\Omega_2 = [2, 5] \times [2, 5]$ and $\Omega_3 = [5, 10] \times [0, 2]$, respectively in the unbiased (left) and biased (right) cases. We note that each domain contains one of the three equilibrium points and thus we can refer to ρ_1 and ρ_3 as the probabilities of each decision states and to ρ_2 as the probability of the spontaneous state. The initial condition we consider implies $\rho_1(0) = \rho_3(0) \simeq 0$ and $\rho_2(0) \simeq 1$. Moreover, in the unbiased case, the symmetry of the problem leads to $\rho_1(t) = \rho_3(t)$ for every $t \geq 0$, i.e., the two decision states are taken with equal probability. However, in the biased case, ρ_3 remains very small and the decision state S_1 is obtained with a probability almost equal to 1.

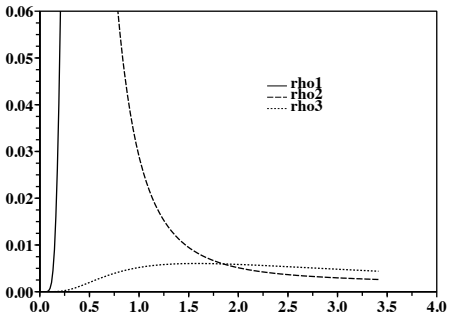

Fig. 6 Zoom in of the densities in the biased case

In figure 6 we show a zoom for the ρ_i densities of the biased case. We can see that ρ_3 rises up in the first seconds, and then slowly decreases. Letting the computation evolving for a longer time the density ρ_3 will converge to zero. But this will take a very long time due to the metastability of the system.

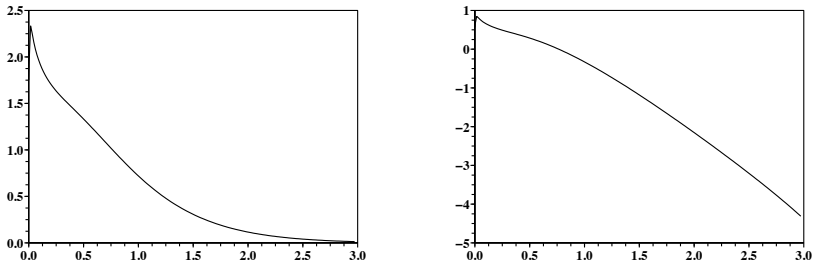

Fig. 7 Convergence toward the stationary solution, in the unbiased case. Right: in logarithmic scale

In figure 7 we show the convergence of the solution of the Fokker-Planck equation to its stationary state in L^2 norm. On the left we present the convergence with respect to time and on the right the same result but in logarithmic scale. We remark that a linear regression done on the second half of the curve has a slope of -0.19 with a standard deviation of 0.031, and a linear regression done on the last quarter of the curve has a slope of -0.08 with a standard deviation of 0.004. This means that after a small transition period, the convergence of the solution towards its stationary state has an exponential behavior. This estimate of the slope of the trend to equilibrium, denoted by Θ later on, helps obtain a direct estimate of the reaction time. We may define the reaction time as the time for stabilization to achieve certain threshold or tolerance. For

instance, we can define it as the time such that:

$$\max\left(|\rho_1(t)-\rho_1(\infty)|, |\rho_3(t)-\rho_3(\infty)|\right) \leq \|p(t)-p_\infty\|_{L^1(\Omega)} \simeq Ce^{-\Theta t} \leq \text{Tol}.$$

Finally, we perform a different numerical test, intended to be a first step in the study of the escaping time problem (or first passage problem). We consider only the unbiased case, because we know that for a time large enough the probability function p must be distributed in equal parts on both the domains Ω_1 and Ω_3, no matter the initial condition. We let the diffusion coefficient β vary in the set $(0.2, ..., 1)$, see table 1, and choose as initial data a Gaussian distribution centered near the stable point S_1, hence in the domain Ω_1. We then stop the numerical simulation when half of the mass has arrived in the Ω_3 domain, that is when $\rho_1(T) < 2\rho_3(T)$. We shall call escaping time, the smallest time T at which the above condition is verified. In table 1, we give the values of the escaping time T (expressed in seconds) for different values of the diffusion coefficient β. As one may expect, the bigger the diffusion coefficient, the smaller the escaping time T.

Table 1 Escaping Time.

β	0.2	0.3	0.4	0.5	0.6	0.7	0.8	0.9	1
T	12.91	3.33	1.70	1.12	0.80	0.60	0.49	0.37	0.30

It is well known, see for example [14], for one dimensional problems, that the expectation of a first passage problem is given by the Kramers law, $\mathbb{E}(t) = \exp\left(H/\beta^2\right)$, where H represents the potential gap and β the diffusion coefficient.

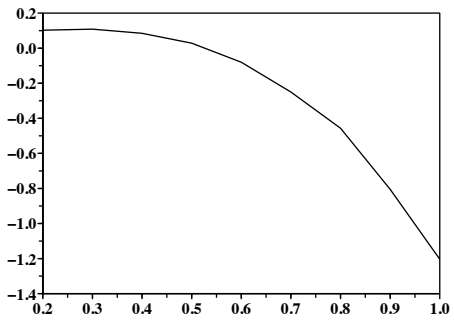

Fig. 8 The value $\beta^2 \log(T)$ with respect to the diffusion coefficient β in log scale. When β goes to zero, the value converges to 0.1.

In figure 8 we plot the value of $\beta^2 \log(T)$ with respect to β. We observe that, when β goes to zero, this value has a finite limit (close to 0.1). Hence,

we can deduce an exponential behavior for the escaping time. In the potential flux situation the above limit corresponds to the maximal bound of the potential gap, H. Let us recall that in our case the flux F is not the gradient of a potential. This kind of behavior (exponential decay of the escaping time versus the noise) has been proved also for some particular multi-dimensional problems. Nevertheless, to our knowledge, there is no proof that for general multi-dimensional problems the expectation of the escaping time has such an exponential behaviour.

3 Existence, Uniqueness and Asymptotic Stability of the Stationary Solution

In this section we first study the existence, uniqueness and positivity of the solution of the associated stationary problem, see subsection 3.1. Then we prove the existence and uniqueness of the solution for the evolutionary Fokker-Planck model (7)-(8), see subsection 3.2. Finally, in subsection 3.3, within the framework of the general relative entropy theory [18,19], we show the decay of the relative entropy. As a consequence, we can prove the convergence of the solution of (7)-(8) towards the unique positive normalized solution of the stationary problem associated to it.

Let us set the notation for this section. We will first assume we have a bounded domain $\Omega \subset \mathbb{R}^2$ for which the divergence theorem and the standard trace theorems for Sobolev functions, for instance the embedding from $H^2(\Omega)$ onto $H^{3/2}(\partial\Omega)$, are valid. Moreover, we need the strong maximum principle to apply, and thus, we will assume $\Omega \in C^2$. Obviously, this is not true for square like domains as in the computational neuroscience model at the origin of this work. However, it is true for smooth approximations of rectangular domains which avoid the corners in the domain of interest. As announced, we assume that the flux function satisfies

$$F \in C^1(\bar{\Omega}, \mathbb{R}^2) \quad \text{with} \qquad F \cdot n < 0 \quad \text{on } \partial\Omega, \tag{10}$$

being n the outwards unit normal to $\partial\Omega$.

Let us, define the following linear operator $\mathcal{A}$, for every given $u \in H^2(\Omega)$:

$$\mathcal{A}u = -\frac{\beta^2}{2}\Delta u + \nabla \cdot (Fu).$$

Then, the Fokker-Planck problem (7)-(8) for the distribution function $p(t, \nu)$ is just a particular case of the general Fokker-Planck equation for $u(\nu, t)$ with non-gradient drift that reads:

$$\begin{cases} \dfrac{\partial u}{\partial t} + \mathcal{A}u = 0 \quad \text{in } \Omega \times (0,T) \\ \left(Fu - \dfrac{\beta^2}{2}\nabla u\right) \cdot n = 0 \quad \text{on } \partial\Omega \times (0,T) \end{cases}, \tag{11}$$

and we endow the parabolic system (11) by the initial condition $u(\cdot,0) = u_0(\cdot) \in L^2(\Omega)$.

Concerning the stationary problem associated with (11), in subsection 3.1 we will consider the elliptic problem:

$$\begin{cases} \mathcal{A}u + \xi u = f \quad \text{in } \Omega \\ \left(Fu - \dfrac{\beta^2}{2}\nabla u\right)\cdot n = 0 \quad \text{on } \partial\Omega\,, \end{cases} \tag{12}$$

with f a given function in $L^2(\Omega)$ and $\xi \in \mathbb{R}$ conveniently chosen, under the assumptions (10) and (5).

Finally, in subsection 3.3 we deal with problem (11), and its dual form:

$$\begin{cases} \dfrac{\partial v}{\partial t} = -F\cdot\nabla v + \dfrac{\beta^2}{2}\Delta v, \quad \text{in } \Omega\times(0,T) \\ \dfrac{\partial v}{\partial n} = 0, \qquad\qquad\qquad \text{on } \partial\Omega\times(0,T) \end{cases} \tag{13}$$

associated to the initial conditions: $v_0(\cdot) = v(0,\cdot)$.

3.1 Stationary problem

We consider here the stationary problem (12) and the bilinear form associated with $\mathcal{A}$:

$$a(u,v) = \int_\Omega \frac{\beta^2}{2}\nabla u\cdot\nabla v\, d\nu - \int_\Omega uF\cdot\nabla v\, d\nu\,, \quad \forall\, u,v\in H^1(\Omega)\,. \tag{14}$$

It is easy to check that:

Lemma 1 *The bilinear form $a(u,v)$ satisfies:*

i. $a(u,v)$ is continuous:

$$|a(u,v)| \le M||u||_{H^1}||v||_{H^1}\,, \quad \forall\, u,v\in H^1(\Omega),$$

with $M = \frac{\beta^2}{2} + ||F||_\infty$.

ii. $a(u,v)$ is "coercive", that is, it verifies:

$$a(u,u) + \rho||u||^2_{L^2} \ge \theta||u||_{H^1} \quad \forall\, u\in H^1(\Omega)\,,$$

with $\rho = C+\theta$ with $C = \dfrac{1}{\sqrt{2}\beta^2}$ and $\theta = \beta^2/4$.

Proof. i. We have, from (14):

$$|a(u,v)| \leq \frac{\beta^2}{2}\int_\Omega |\nabla u||\nabla v|\,d\nu + \|F\|_\infty \int_\Omega |u|\,|\nabla v|\,d\nu \leq$$
$$\leq \left(\frac{\beta^2}{2} + \|F\|_\infty\right)\|u\|_{H^1}\|v\|_{H^1},$$

where $||F||_\infty$ corresponds to the maximum of $|F|$ in $\bar{\Omega}$.

ii. We have, from (14):

$$\frac{\beta^2}{2}\int_\Omega |\nabla u|^2\,d\nu \leq a(u,u) + \|F\|_\infty \int_\Omega |u||\nabla u|\,d\nu.$$

Now, from the following inequality $ab \leq \varepsilon a^2 + b^2/4\varepsilon$, with $a, b, \varepsilon > 0$, we get:

$$\int_\Omega |\nabla u||u|\,d\nu \leq \varepsilon \int_\Omega |\nabla u|^2\,d\nu + \frac{1}{4\varepsilon}\int_\Omega |u|^2\,d\nu.$$

Then choosing ε so small that: $\varepsilon\|F\|_\infty \leq \beta^2/4$, e.g. $\varepsilon = \frac{\beta^2}{8\|F\|_\infty}$ we have:

$$\frac{\beta^2}{4}\int_\Omega |\nabla u|^2\,d\nu \leq a(u,u) + C\int_\Omega |u|^2\,d\nu$$

with

$$C = \frac{1}{\sqrt{2}\beta^2}.$$

Finally, from this we obtain:

$$a(u,u) + \left(C + \frac{\beta^2}{4}\right)||u||^2_{L^2} \geq \frac{\beta^2}{4}||u||^2_{H^1},$$

which ends the proof. □

Lemma 2 *For each $f \in L^2(\Omega)$, problem (12) has an unique solution in $H^2(\Omega)$ for $\xi \geq \rho$.*

Proof. Applying Lemma 1 we have that $a(u,v) + \xi\langle u, v\rangle_{L^2}$ is continuous and coercive, for $\xi \geq \rho$. Then, applying Lax-Milgram theorem, we have that, for each $f \in L^2(\Omega)$, there exists an unique $u \in H^1(\Omega)$ such that, $\forall\, v \in H^1(\Omega)$:

$$\int_\Omega \left(\frac{\beta^2}{2}\nabla u\cdot\nabla v - uF\cdot\nabla v + \xi uv\right)d\nu = \int_\Omega fv\,d\nu. \tag{15}$$

By regularity, since $f \in L^2(\Omega)$ then we have $u \in H^2(\Omega)$ with traces for u and its derivatives on the boundary. Thus, integrating by parts (15), we get, $\forall v \in H^1(\Omega)$:

$$\int_\Omega \left(\nabla\cdot(Fu) - \frac{\beta^2}{2}\Delta u + \xi u - f\right)v\,d\nu + \int_{\partial\Omega}(Fu - \beta^2\nabla u)\cdot n\,v\,d\sigma = 0. \tag{16}$$

If in (16), we choose $v \in C_c^\infty(\Omega)$, we get in distributional sense:

$$\int_\Omega \left(\nabla \cdot (Fu) - \frac{\beta^2}{2} \Delta u + \xi u - f \right) v \, d\nu = 0 \quad \forall v \in C_c^\infty(\Omega) \, .$$

Hence:

$$\nabla \cdot (Fu) - \frac{\beta^2}{2} \Delta u + \xi u - f = 0 \quad \text{in } L^2(\Omega). \tag{17}$$

Moreover, replacing (17) in (16), we have:

$$\int_{\partial\Omega} \left(Fu - \frac{\beta^2}{2} \nabla u \right) \cdot n \, v \, d\sigma = 0 \, , \forall v \in H^1(\Omega),$$

which implies:

$$\left(Fu - \frac{\beta^2}{2} \nabla u \right) \cdot n = 0 \quad \text{on } \partial\Omega \, ,$$

that is, u satisfies the boundary conditions. □

Let us now define the linear operator:

$$T_\xi : L^2(\Omega) \to L^2(\Omega), \qquad T_\xi f = u, \quad \forall f \in L^2(\Omega) \text{ and } \forall \xi \geq \rho$$

with u the unique solution of (12). In particular, we can prove that:

Lemma 3 *The operator $T_\xi : H^2(\Omega) \to H^2(\Omega)$ is a compact operator for all $\xi \geq \rho$.*

Proof. We have that there exists $u = T_\xi f$ solution of (12), for any $f \in H^2(\Omega)$. By regularity, we have $u \in H^4(\Omega)$ and from the estimate $\|u\|_{H^4(\Omega)} \leq C\|f\|_{H^2(\Omega)}$, we get that T_ξ maps $H^2(\Omega)$ onto itself. Moreover, the compactness of the imbedding, $H^4(\Omega) \hookrightarrow H^2(\Omega)$ implies that T_ξ is a compact operator. □

Consider now the cone K:

$$K = H^2_+(\Omega) = \left\{ u \in H^2(\Omega) \,|\, u(\nu) \geq 0 \ a.e \ \nu \in \Omega \right\},$$

we remark that it has non-empty interior, see [1, Page 360] and it corresponds to everywhere positive functions in Ω. To prove the existence of solution to our problem, we shall use the following theorem derived from the Krein-Rutman theorem:

Theorem 1 (Krein-Rutman) *Let X be a Banach space, $K \subset X$ a solid cone (i.e the cone has non-empty interior K^0), $T : X \to X$ a compact linear operator which is strongly positive, i.e, $Tf \in K^0$ if $f \in K \backslash \{0\}$. Then, $r(T) > 0$, and $r(T)$ is a simple eigenvalue with an eigenvector $v \in K^0$; there is no other eigenvalue with positive eigenvector.*

Lemma 4 *The operator T_ξ is strongly positive in $H^2_+(\Omega)$ under the assumption $\xi \geq \max(\rho, \|(\nabla \cdot F)^-\|_{L^\infty(\Omega)})$.*

Proof. We first start by defining the operator L as follows:

$$Lu = \mathcal{A}u + \xi u\,,$$

then, $Lu = f \geq 0$ if $u = T_\xi f$. Under the assumptions on ξ, we have that the operator has a zero order term given by $\xi + \nabla \cdot F \geq 0$ on Ω. Thus, we can apply the weak maximum principle to L, see [13, page 329] deducing that

$$\min_{\nu \in \bar{\Omega}} u = - \max_{\nu \in \partial\Omega} u^-.$$

Now, assume that the minimum of u in Ω is negative, then it is achieved at a $\nu_0 \in \partial\Omega$ such that $u(\nu_0) < 0$. Using (10) we get

$$\frac{\beta^2}{2}\frac{\partial u}{\partial n}(\nu_0) = u(\nu_0) F \cdot n > 0\,,$$

contradicting the fact that ν_0 is a minimum at the boundary. Thus, we have proved $u \geq 0$ and that T_ξ maps nonnegative functions into itself: $T_\xi : H^2_+(\Omega) \to H^2_+(\Omega)$.

Suppose now $f \in K\backslash\{0\}$ and $u = T_\xi f$. Moreover, if there exists $\nu_0 \in \Omega$, such that $u(\nu_0) = 0$, then

$$\min_{\Omega} u = u(\nu_0) = 0,$$

because $u(\nu) \geq 0$, $\forall \nu \in \Omega$. Therefore, by the strong maximum principle, we have $u = C$ constant and thus, $u = 0$. This is a contradiction because $f \neq 0$. Then, we have

$$u(\nu) > 0\,, \quad \forall \nu \in \Omega.$$

Consider now $\nu_0 \in \partial\Omega$, we will prove that $u(\nu_0) > 0$. If $u(\nu_0) = 0$, then it is a strict minimum of u at the boundary, and thus

$$\frac{\partial u}{\partial n}(\nu_0) < 0.$$

by Hopf's lemma [13, page 330]. Using (10), we have

$$\frac{\beta^2}{2}\frac{\partial u}{\partial n}(\nu_0) = u(\nu_0) F \cdot n = 0,$$

which is in contradiction. Thus, $u(\nu) > 0$, $\forall \nu \in \bar{\Omega}$, i.e. $u \in K^0$. □

We can now prove the main theorem :

Theorem 2 *Under assumptions (10), there exists an unique probability density function $u_\infty \in H^4(\Omega)$, $u_\infty(\nu) > 0$ in $\bar{\Omega}$ satisfying:*

$$\begin{cases} \mathcal{A}u = 0 \quad \text{in } \Omega \\ \left(Fu - \dfrac{\beta^2}{2}\nabla u\right) \cdot n = 0 \quad \text{on } \partial\Omega \end{cases}. \tag{18}$$

Proof. (a) **Existence and positivity**
Using Lemma 3 and 4, we have that T_ξ satisfies the hypothesis in Theorem 1 for ξ large enough. Therefore, $r(T_\xi) > 0$ and there exists a positive eigenvector v such that $T_\xi v = r(T_\xi)v$, i.e.,

$$\mathcal{A}(r(T_\xi)v) + \xi\, r(T_\xi)v = v.$$

Let $u = r(T_\xi)v$, then u satisfies the boundary conditions in (12) and,

$$\mathcal{A}u + \xi u = \lambda u \quad \text{with } \lambda = \frac{1}{r(T_\xi)}\,.$$

equivalent to,

$$\mathcal{A}u = (\lambda - \xi)u. \tag{19}$$

Multiplying by $\varphi \in H^1(\Omega)$ on both sides of (19) and integrating by parts, we obtain:

$$\int_\Omega \frac{\beta^2}{2}\nabla u \cdot \nabla\varphi \, d\nu - \int_\Omega uF \cdot \nabla\varphi \, d\nu = (\lambda - \xi)\int_\Omega u\varphi \, d\nu.$$

Then, choosing $\varphi = 1$, we get:

$$(\lambda - \xi)\int_\Omega u \, d\nu = 0.$$

But $u > 0$, because $u = r(T_\xi)v > 0$, thus $\xi = \lambda = \frac{1}{r(T_\xi)}$. Therefore, the existence and positivity of a stationary state, i.e., $\mathcal{A}u = 0$ are obtained, since we can choose any multiple of u, we take the one satisfying the normalization condition (5).

(b) **Uniqueness**
Let $u_1 > 0$ satisfies (18). By standard regularity theory, $u_1 \in H^2(\Omega)$ and then $u_1 \in K$. Hence, we have:

$$\mathcal{A}u_1 + \xi u_1 = \frac{1}{r(T_\xi)}u_1$$

by recalling that $\xi = \frac{1}{r(T_\xi)}$. This implies $\mathcal{A}(r(T_\xi)u_1) + \xi r(T_\xi)u_1 = u_1$. On the other hand, by definition of T_ξ, we also have $\mathcal{A}(T_\xi u_1) + \xi T_\xi u_1 = u_1$. Therefore, $T_\xi u_1 = r(T_\xi)u_1$.

Recalling that $r(T_\xi)$ is a simple eigenvalue, we obtain $u_1 = cu$. By means of the normalization hypothesis (5), we finally prove the uniqueness of the solution. By Hopf's Lemma proceeding as in the last part of Lemma 4, we deduce the strict positivity of u_∞. □

3.2 Time evolution problem

Let us first consider the bilinear form associated to $\mathcal{A}$:

$$a(t,u,v) = \int_\Omega \frac{\beta^2}{2}\nabla u \cdot \nabla v \, d\nu - \int_\Omega uF \cdot \nabla v \, d\nu \,, \quad \forall\, u,v \in H^1(\Omega)\,, \tag{20}$$

It is easy to check that :

i. Let $T \in \mathbb{R}_+^*$, then the mapping $t \mapsto a(t,u,v)$ is measurable on $[0,T]$, for fixed $u,v \in H^1(\Omega)$ since it is constant in time.
ii. The bilinear form $a(t,u,v)$ is continuous:

$$|a(t,u,v)| \leq M||u||_{H^1}||v||_{H^1}\,, \quad \forall\, t \in [0,T],\ u,v \in H^1(\Omega)\,,$$

and coercive

$$a(t,u,u) + \rho||u||_{L^2}^2 \geq \theta||u||_{H^1} \quad \forall\, t \in [0,T],\ u \in H^1(\Omega)$$

with $M > 0$, θ and ρ given in Lemma 1.

We say that u is a weak solution of (11) if $u \in L^2(0,T;H^1(\Omega))$ and satisfies:

$$\frac{d}{dt}\int_\Omega uv \, d\nu + a(t,u,v) = \int_\Omega fv \, d\nu. \tag{21}$$

Theorem 3 *Problem (11) has an unique strong solution.*

Proof. The existence of an unique weak solution to (11) is proved applying [26, Theorem 27.3]. Moreover, the weak solution u belongs to $L^2(0,T;H^2(\Omega))$, see [26, Theorem 27.5]. Now, integrating by parts (21), with $f = 0$, we get:

$$\int_\Omega \left(\frac{\partial u}{\partial t} - \frac{\beta^2}{2}\Delta u + \nabla\cdot(Fu)\right) v \, d\nu + \int_{\partial\Omega}\left(Fu - \frac{\beta^2}{2}\nabla u\right)\cdot n\, v \, d\sigma = 0\,, \tag{22}$$

for all $v \in H^1(\Omega)$. Choosing $v \in C_c^\infty(\Omega)$, we obtain, in the distributional sense:

$$\frac{\partial u}{\partial t} - \frac{\beta^2}{2}\Delta u + \nabla\cdot(Fu) = 0, \tag{23}$$

which is equivalent to $\partial_t u + \mathcal{A}u = 0$. Finally, replacing (23) in (22), we have:

$$\int_{\partial\Omega}\left(Fu - \frac{\beta^2}{2}\nabla u\right)\cdot n\, v \, d\sigma = 0 \qquad \forall\, v \in H^1(\Omega),$$

yielding to: $\left(Fu - \frac{\beta^2}{2}\nabla u\right)\cdot n = 0$ on $\partial\Omega$. Hence the weak solution u is in fact a strong solution. □

Concerning the positivity of the solution of (11), we remark that since the flux F has negative divergence, the maximum principle does not hold in our case. Nevertheless, it is possible to prove the positivity for the solution using the relative entropy decay, as shown in the next section. Concerning the dual problem (13), it is a standard evolution problem with Neumann boundary conditions for which classical references apply, see [13].

3.3 Convergence to steady state

In order to show the positivity of the solution of problem (11) and the convergence to the stationary solution, u_∞ of problem (18), we need to prove the decay of the relative entropy, see [19]. We will hence consider problems (11) and (13). We first prove the following conservation result:

Lemma 5 *Given any strong solution of (11) with normalized initial data, then the solution satisfies mass conservation, that is:*

$$\int_\Omega u(t,\nu)\,d\nu = \int_\Omega u_0(\nu)\,d\nu = 1. \tag{24}$$

Proof. Let us consider the product of u and v, respectively solutions to (11) and (13). Integrating over the phase space Ω the derivative in time of uv, and using (11) and (13), we get:

$$\begin{aligned}\frac{d}{dt}\int_\Omega uv\,d\nu &= -\int_\Omega \left(-Fu+\frac{\beta^2}{2}\nabla u\right)\cdot\nabla v\,d\nu + \int_\Omega u\frac{\partial v}{\partial t}\,d\nu = \\ &= \int_\Omega uF\cdot\nabla v\,d\nu - \frac{\beta^2}{2}\int_\Omega u\Delta v\,d\nu + \int_\Omega u\frac{\partial v}{\partial t}\,d\nu = 0.\end{aligned}$$

Hence,

$$\int_\Omega uv\,d\nu = \int_\Omega u_0v_0\,d\nu$$

and the result follows by considering that constant functions are solutions of (13). □

Given any convex function $H = H(\omega)$, where $\omega = u_2/u_1$ and u_1 and u_2 are strong solutions of (11) with $u_1 > 0$ in $\bar\Omega$, we have the following:

Lemma 6 *For any u_1 and u_2 strong solutions of (11), and v strong solution of (13) with $u_1, v > 0$ in $\bar\Omega$, then:*

$$\begin{aligned}\frac{d}{dt}\left[vu_1H(\omega)\right] = \frac{\beta^2}{2}&\left(\nabla\cdot\left[v^2\nabla\left(\frac{u_1}{v}H(\omega)\right)\right] - vu_1H''(\omega)\left|\nabla(\omega)\right|^2\right)\\ &-\nabla\cdot\left[Fvu_1H(\omega)\right]\end{aligned} \tag{25}$$

Proof. Let us develop the left hand side of (25), using (11) and (13):

$$\begin{aligned}\frac{d}{dt}\left[vu_1H(\omega)\right] = &-\nabla\cdot\left[Fu_1vH(\omega)\right] + u_1F\cdot\nabla\left(vH(\omega)\right)\\ &-u_1H(\omega)F\cdot\nabla v + \frac{u_2}{u_1}vH'(\omega)\nabla\cdot(u_1F)\\ &-vH'(\omega)\nabla\cdot(u_2F) - \frac{\beta^2}{2}u_1H(\omega)\Delta v\\ &+\frac{\beta^2}{2}\left[vH(\omega) - \frac{u_2}{u_1}vH'(\omega)\right]\Delta u_1 + \frac{\beta^2}{2}vH'(\omega)\Delta u_2\,.\end{aligned}$$

We separate now the computation in two parts: the one concerning first order derivatives (I) and the one concerning second order derivatives (II). We start by computing (I). Leaving the first term unchanged and developing the following ones, we get:

$$\begin{aligned}(I) = &-\nabla\cdot\left[Fu_1vH\left(\omega\right)\right]+u_1H\left(\omega\right)F\cdot\nabla v\\&+vH'\left(\omega\right)F\cdot\left(\nabla u_2-\frac{u_2}{u_1}\nabla u_1\right)-u_1H\left(\omega\right)F\cdot\nabla v\\&+\frac{u_2}{u_1}vH'\left(\omega\right)\nabla u_1\cdot F+vH'\left(\omega\right)u_2\nabla\cdot F\\&-vH'\left(\omega\right)\nabla u_2\cdot F-vH'\left(\omega\right)u_2\nabla\cdot F=-\nabla\cdot\left[Fu_1vH\left(\omega\right)\right].\end{aligned}$$

Concerning the second part (II), we start developing $\nabla\cdot\left[v^2\nabla\left(\frac{u_1}{v}H\left(\omega\right)\right)\right]$, and find that:

$$\begin{aligned}\nabla\cdot\left[v^2\nabla\left(\frac{u_1}{v}H\left(\omega\right)\right)\right]=&-u_1H\left(\omega\right)\Delta v+\left[vH\left(\omega\right)-\frac{u_2}{u_1}vH'\left(\omega\right)\right]\Delta u_1\\&+vH'\left(\omega\right)\Delta u_2-\nabla vH'\left(\omega\right)\left(\nabla u_2-\frac{u_2}{u_1}\nabla u_1\right)\\&+H'\left(\omega\right)\nabla u_2\cdot\nabla v+vH''\left(\omega\right)\nabla u_2\cdot\nabla\left(\omega\right)\\&-\frac{u_2}{u_1}H'\left(\omega\right)\nabla u_1\cdot\nabla v-\frac{u_2}{u_1}vH''\left(\omega\right)\nabla u_1\cdot\nabla\left(\omega\right).\end{aligned}$$

Multiplying by $\frac{\beta^2}{2}$, recalling part (II) of our development and that $u_1\nabla\left(\omega\right)=\nabla u_2-\frac{u_2}{u_1}\nabla u_1$, we then get:

$$\frac{\beta^2}{2}\nabla\cdot\left[v^2\nabla\left(\frac{u_1}{v}H\left(\omega\right)\right)\right]=(II)+\frac{\beta^2}{2}vu_1\left|\nabla\left(\omega\right)\right|^2H''\left(\omega\right),$$

which completes the proof in the case H is smooth. □

Let us now define the relative entropy operator:

$$\mathcal{H}_v(u_2|u_1)=\int_\Omega vu_1H\left(\omega\right)\,d\nu \tag{26}$$

and the decay operator:

$$\mathcal{D}_v(u_2|u_1)=\int_\Omega vu_1H''\left(\omega\right)\left|\nabla\left(\frac{u_2}{u_1}\right)\right|^2\,d\nu. \tag{27}$$

Then we have the following:

Theorem 4 *For any u_1 and u_2 strong solutions of (11), and v strong solution of (13) with $u_1,v>0$ in $\bar{\Omega}$, if H is a smooth convex function then, the relative entropy is decreasing in time and*

$$\frac{d}{dt}\mathcal{H}_v(u_2|u_1)=-\frac{\beta^2}{2}\mathcal{D}_v(u_2|u_1)\leq 0. \tag{28}$$

Proof. Integrating (25) over the domain Ω, we get:

$$\frac{d}{dt}\int_{\Omega} vu_1 H(\omega)\, d\nu = -\frac{\beta^2}{2}\int_{\Omega} vu_1 H''(\omega)\left|\nabla(\omega)\right|^2 d\nu - \int_{\partial\Omega}(F\cdot n)vu_1 H(\omega)\, d\sigma + \frac{\beta^2}{2}\int_{\partial\Omega} v^2\nabla\left(\frac{u_1}{v}H(\omega)\right)\cdot n\, d\sigma\,.$$

We just have to show that the integration on the boundaries are equal to zero. Developing the last term, we get:

$$\int_{\partial\Omega}(F\cdot n)vu_1 H(\omega)\, d\sigma + \frac{\beta^2}{2}\int_{\partial\Omega} v^2\nabla\left(\frac{u_1}{v}H(\omega)\right)\cdot n\, d\sigma = \int_{\partial\Omega}(F\cdot n)vu_1 H(\omega) + \frac{\beta^2}{2}\frac{\partial u_1}{\partial n}vH(\omega)\, d\sigma + \int_{\partial\Omega}\frac{\beta^2}{2}u_1\frac{\partial v}{\partial n}H(\omega) + \frac{\beta^2}{2}vH'(\omega)\,u_1\frac{\partial\omega}{\partial n}\, d\sigma.$$

Then, applying boundary conditions in (11) and (13), we have:

$$(F\cdot n)vu_1 H(\omega) - \frac{\beta^2}{2}\frac{\partial u_1}{\partial n}vH(\omega) = 0,$$

$$\frac{\beta^2}{2}u_1\frac{\partial v}{\partial n}vH(\omega) = 0.$$

Finally, recalling that $\omega = u_2/u_1$, that from (11) we have

$$F\cdot n = \frac{\beta^2}{2}\frac{1}{u_1}\frac{\partial u_1}{\partial n},$$

and applying (13), we obtain:

$$\int_{\partial\Omega}\frac{\beta^2}{2}vH'(\omega)\,u_1\frac{\partial\omega}{\partial n}\, d\sigma = \int_{\partial\Omega}\frac{\beta^2}{2}\left(vH'(\omega)\frac{\partial u_2}{\partial n} - vH'(\omega)\frac{\partial u_1}{\partial n}\frac{u_2}{u_1}\right) d\sigma =$$

$$\int_{\partial\Omega}\frac{\beta^2}{2}vH'(\omega)\frac{\partial u_2}{\partial n} - vH'(\omega)\,(F\cdot n)u_2\, d\sigma = 0,$$

and the theorem is proved. □

We can now prove the positivity of the solution of the evolution problem for the linear Fokker-Planck equation (11).

Theorem 5 *If u_0 is nonnegative, then the solution u of problem (11) is nonnegative.*

Proof. Consider the operators (26) and (27), and let u_1 be the stationary solution u_∞ of problem (12), and v a positive constant, say $v = 1$. We recall that, $u_\infty > 0$ in $\bar{\Omega}$ and that constants are solution to (13). Moreover, let $H(\omega) = \omega^-$, the negative part of ω, $\omega^- = max(-\omega, 0)$. Then $H(\omega)$ is a positive and convex function than can be approximated easily by smooth convex positive functions $H_\delta(\omega)$. Thus, we can obtain

$$\frac{d}{dt}\int_\Omega u_\infty H_\delta\left(\frac{u_2}{u_\infty}\right)\,d\nu \le 0.$$

and by approximation $\delta \to 0$, we deduce

$$h(t) := \int_\Omega u_\infty H\left(\frac{u_2(t,\nu)}{u_\infty}\right)\,d\nu \le \int_\Omega u_\infty H\left(\frac{u_2(0,\nu)}{u_\infty}\right)\,d\nu\,, \tag{29}$$

for all $t \ge 0$. Here, u_2 is any solution of (11) endowed by the positive initial condition $u_2(t = 0, \nu_1, \nu_2) = u_0(\nu_1, \nu_2) \ge 0$. Hence, the function $h(t) \ge 0$ is decreasing in time, because of (29), and at the initial time $t = 0$, $h(0) = 0$. Therefore, $h(t) = 0$ for all $t \ge 0$, and, as u_∞ is positive, u_2 must be nonnegative. □

The consequences of the existence of this family of Liapunov functionals given in Theorem 4 for (11) have already been explored for several equations in [18,19] where they have been called general relative entropy (GRE) inequalities. The same conclusions apply here.

Corollary 1 *Given F satisfying (10) and any solution u with normalized initial data u_0 to (11), then the following properties hold:*

i) Contraction principle:

$$\int_\Omega |u(t,\nu)|\,d\nu \le \int_\Omega |u_0(\nu)|\,d\nu. \tag{30}$$

ii) L^p bounds, $1 < p < \infty$:

$$\int_\Omega u_\infty(\nu)\left|\frac{u(t,\nu)}{u_\infty(\nu)}\right|^p\,d\nu \le \int_\Omega u_\infty(\nu)\left|\frac{u_0(\nu)}{u_\infty(\nu)}\right|^p\,d\nu. \tag{31}$$

iii) Pointwise estimates:

$$\inf_{\nu\in\Omega}\frac{u_0(\nu)}{u_\infty(\nu)} \le \frac{u(t,\nu)}{u_\infty(\nu)} \le \sup_{\nu\in\Omega}\frac{u_0(\nu)}{u_\infty(\nu)}\,. \tag{32}$$

This corollary is a consequence of the GRE inequality in Theorem 4 with $H(s) = |s|$, $H(s) = |s|^p$, and $H(s) = (s-k)_+^2$ respectively by approximation from smooth convex functions. Moreover, the GRE inequality gives the convergence of the solution $u(t)$ to the stationary state u_∞.

Corollary 2 (Long time asymptotic) *Given F satisfying (10) and any solution u with normalized initial data u_0 to (11), then*

$$\lim_{t\to\infty}\int_\Omega |u(t,\nu)-u_\infty(\nu)|^2\,d\nu = 0\,. \tag{33}$$

Proof. Using the general entropy inequality with $H(s)=s^2/2$ and $v=1$, we get from Theorem 4 that

$$\int_\Omega \frac{u(T,\nu)^2}{u_\infty(\nu)}\,d\nu + 2\int_0^T\int_\Omega u_\infty(\nu)\left|\nabla\left(\frac{u(t,\nu)}{u_\infty(\nu)}\right)\right|^2 d\nu\,dt \le \int_\Omega \frac{u_0(\nu)^2}{u_\infty(\nu)}\,d\nu\,, \tag{34}$$

for all $T>0$. From (34), we deduce that

$$\int_0^\infty\int_\Omega u_\infty(\nu)\left|\nabla\left(\frac{u(t,\nu)}{u_\infty(\nu)}\right)\right|^2 d\nu\,dt < \infty\,,$$

and thus, there exits $\{t_n\}\nearrow\infty$ such that for any fixed $T>0$

$$\int_{t_n}^{t_n+T}\int_\Omega u_\infty(\nu)\left|\nabla\left(\frac{u(t,\nu)}{u_\infty(\nu)}\right)\right|^2 d\nu\,dt\to 0 \qquad \text{as } n\to\infty.$$

Now, developing the square, we deduce

$$\begin{aligned}\int_\Omega u_\infty\left|\nabla\left(\frac{u(t)}{u_\infty}\right)\right|^2 d\nu &= \int_\Omega\left(\frac{|\nabla u(t)|^2}{u_\infty} - 2\frac{\nabla u(t)\cdot\nabla u_\infty}{u_\infty^2}u(t)\right.\\ &\qquad \left.+\frac{|\nabla u_\infty|^2}{u_\infty^3}u(t)^2\right)d\nu\\ &= \int_\Omega\left(\frac{|\nabla u(t)|^2}{u_\infty}+\frac{|\nabla u_\infty|^2}{u_\infty^3}u(t)^2\right)d\nu\\ &\qquad +\int_\Omega u(t)^2\nabla\cdot\left(\frac{\nabla u_\infty}{u_\infty^2}\right)d\nu - \int_{\partial\Omega}\frac{u(t)^2}{u_\infty^2}\frac{\partial u_\infty}{\partial n}d\sigma\end{aligned} \tag{35}$$

where an integration by parts has been done in the last term. Taking into account that the stationary solution $u_\infty\in H^4(\Omega)$ and that is strictly positive, from Theorem 2, we get that u_∞ and their derivatives up to second order are in $C(\bar\Omega)$ with u_∞ bounded away from zero. From this fact together with the boundary condition

$$\frac{\beta^2}{2}\frac{\partial u_\infty}{\partial n} = u_\infty(F\cdot n),$$

and the L^2 estimates in (31), we conclude that there exists a constant depending only on F, u_0 and u_∞ such that the terms

$$\int_{\partial\Omega}\frac{u(t)^2}{u_\infty^2}\frac{\partial u_\infty}{\partial n}d\sigma, \qquad \int_\Omega u(t)^2\nabla\cdot\left(\frac{\nabla u_\infty}{u_\infty^2}\right)d\nu,$$

and

$$\int_\Omega\frac{|\nabla u_\infty|^2}{u_\infty^3}u(t)^2\,d\nu$$

are uniformly bounded in $t \geq 0$. This implies immediately that

$$\int_{t_n}^{t_n+T} \int_\Omega \frac{|\nabla u(t)|^2}{u_\infty} \, d\nu \, dt$$

is uniformly bounded in n. Therefore, defining the sequence $u_n(t,\nu) := u(t + t_n, \nu)$ for all $t \in [0,T]$ and $\nu \in \Omega$, we deduce that $u_n \in L^2(0,T;H^1(\Omega))$ uniformly bounded in n since u_∞ is bounded away from zero. Using this fact and the L^2-bounds in (31), we can come back to the equation satisfied by $u(t)$ and check that $\frac{\partial u_n}{\partial t} \in L^2(0,T;H^{-1}(\Omega))$ uniformly in n. The standard Aubin-Lions's compactness lemma implies the existence of a subsequence, denoted with the same index, such that $u_n \to u_*$ strongly in $L^2(0,T;L^2(\Omega))$ and weakly in $L^2(0,T;H^1(\Omega))$.

From (35), we can easily deduce that

$$\begin{aligned} 0 &\leq \int_0^T \int_\Omega u_\infty(\nu) \left| \nabla \left(\frac{u_*(t,\nu)}{u_\infty(\nu)} \right) \right|^2 d\nu \, dt \\ &\leq \liminf_{n\to\infty} \int_0^T \int_\Omega u_\infty(\nu) \left| \nabla \left(\frac{u_n(t,\nu)}{u_\infty(\nu)} \right) \right|^2 d\nu \, dt \to 0 \qquad \text{as } n \to \infty \,, \end{aligned}$$

and thus, u_*/u_∞ is constant. Due to the normalisation condition in (24), then $u_* = u_\infty$. Since the limit is the same for all subsequences, we deduce the desired claim. □

Remark 2 (Splitting and Rate of Convergence) We finally remark that, even if the flux F is not in a gradient form, following [2,3,4], once we have the existence, uniqueness and positivity for the solution u_∞ to the stationary problem associated to (7), we may split the flux F into a gradient part plus a non gradient one. In fact, let A be defined by $A = -\log u_\infty$, so that $e^{-A} = u_\infty$ is the solution of the stationary problem associated to (7). Then we have:

$$\nabla \cdot \left(F e^{-A} + \frac{\beta^2}{2} \nabla A e^{-A} \right) = 0 \,,$$

or equivalently

$$\nabla \cdot \left(\left(F + \frac{\beta^2}{2} \nabla A \right) e^{-A} \right) = 0 \,,$$

Defining $G = (F + \frac{\beta^2}{2}\nabla A)$, we have split F as $F = -\frac{\beta^2}{2}\nabla A + G$. In particular, we note that G is such that $\nabla \cdot (G e^{-A}) = 0$, but we do not have yet an explicit form for G. Once this splitting is done, a variation of entropy-entropy dissipation arguments as in [5, Subsection 2.4] in bounded domains with the no-flux boundary conditions should lead to an exponential rate of convergence under the assumption that the hessian matrix of A, D^2A, is positive definite with an explicit rate given by the minimum eigenvalue of D^2A. However, we do not know under which assumptions we can show that the hessian matrix of the potential A is positive definite or equivalently that u_∞ is log-concave. It is worthy to mention that the Krein-Rutman theorem used shows that all other eigenvalues of problem (12) are negative but no general conditions on the explicit form of F to measure the spectral gap are known to our knowledge.

4 Conclusions

In this paper, we have presented a kinetic description of a stochastic system of differential equations, see [11], describing the behaviour of two interacting populations of neurons under the action of two possibly different stimuli. The analysis is based on the Fokker-Planck equation associated to a stochastic differential system modeling the firing rates of the two neuron populations. An important feature of our model is that the flux term in the Kolmogorov equation is not the gradient of a potential function. This implies that we do not have explicit solutions.

Performing a classic finite difference discretization scheme, on one hand we obtain the same results as in [11], and additionally, we give the temporal evolution of each population and the two-dimensional profile of the solutions. The evolution on time highlights that the problem we consider is characterized by a slow-fast behaviour, while the two-dimensional plot shows that the two density picks are aligned along a curve, called slow-manifold. Moreover, we numerically show and prove that the decay of the solution to equilibrium has an exponential behaviour. This trend to equilibrium has implications in finding the probability of reaching a decision and the reaction time. Finally, we have performed an "exit time" test, showing the exponential dependence of the exit time with respect to the noise strength β. We remark that due to the expression of the sigmoidal function $\varphi(x)$, we have no explicit information about the speed of the decay to equilibrium, nor about the exit time problem.

One main aspect of our numerical simulations is the long computing-time needed in order to reach equilibrium. This is mainly due to the slow-fast behavior of the stochastic differential system. As explained also in [8], these kinds of problems are characterized by the fast dynamics of a solution towards a curve, on which the behavior becomes slow. We suggest that it is possible to reduce our problem to a one-dimensional model defined on the slow-manifold, i.e. the curve relying the three equilibrium points of the stochastic differential system, see [7]. The same approach was indeed applied on the mutual inhibition model to derive two one-dimensional independent Ornstein-Uhlenbeck equations, see [8]. Nevertheless, in our model, due to the form of the sigmoidal function $\varphi(x)$, we do not have explicit/analytical expressions for this manifold, and all computations and the reduction to the one-dimensional model have to be done numerically. Clearly, for this one-dimensional reduction we will have an explicit expression for the steady state, and also explicit formulations for the exit time problem. Using this reduced model (with a very reduced computational time), it should be possible to investigate in detail the effects of the parameters of the model for the two choices task paradigm of decision making. Since this is beyond the goal of this paper, we shall not detail further this aspect, which we will develop in future work.

Finally, we have rigorously shown this numerically observed stabilization in time of the probability density in the Fokker-Planck setting. We obtained two main mathematical elements, first the existence, uniqueness and positivity of the solution of the time dependent problem, i.e. the well-posedness of the

problem; and second, the convergence in time of this solution to the equilibrium solution, i.e. the solution of the stationary problem. Both these elements are important. The first one ensures that the model makes sense, in fact existence and uniqueness of a positive solution means that given initial data we will have a unique evolution for the probability of neuron populations with a well-defined positive firing rate. The second one shows that the system of neuron populations will reach a unique behaviour if we wait for a long time irrespective of its initial assumption. Obtaining an estimate on the rate of convergence by estimating the first nonzero eigenvalue or spectral gap is an open problem directly related to the reaction time.

Acknowledgements JAC acknowledges partial support from DGI-MICINN (Spain) project MTM2008-06349-C03-03 and 2009-SGR-345 from AGAUR-Generalitat de Catalunya. SC and SM acknowledge support by the ANR project MANDy, Mathematical Analysis of Neuronal Dynamics, ANR-09-BLAN-0008-01. The authors would like to thanks G. Deco and N. Berglund for their many inspiring discussions and the CRM (Centre de Recerca Matemática) in Barcelona where part of this work was done during the thematic program in Mathematical Biology.

References

1. Amann H (1976) Fixed Point Equations and Nonlinear Eigenvalue Problems in Ordered Banach Spaces. SIAM Review, 18(4):620-709.
2. Arnold A, Carlen E (2000) A generalized Bakry-Emery condition for non-symmetric diffusions. EQUADIFF 99 - Proceedings of the Internat. Conference on Differential Equations, Berlin 1999, B. Fiedler, K. Groger, J. Sprekels (Eds.); World Scientific, SIngapore/New Jersey/ Hong Kong :732-734.
3. Arnold A, Carlen E, Ju Q (2008) Large-time behavior of non-symmetric Fokker-Planck type equations. Communications on Stochastic Analysis, 2(1):153-175.
4. Arnold A, Carrillo J A, Manzini C (2010) Refined Long-time Asymptotics for Some Polymeric Fluid flow Models. Comm. Math. Sci., 8:763-782.
5. Arnold A, Markowich P, Toscani G, Unterreiter A (2001) On convex Sobolev inequalities and the rate of convergence to equilibrium for Fokker-Plack type equations. Comm. PDE, 26:43-100.
6. Attneave F (1971) Multistability in perception. Sci. Am., 225:63-71.
7. Berglund N, Gentz B (2005) Noise-Induced Phenomena in Slow-Fast Dynamical Systems. A Sample-Paths Approach. Springer, Probability and its Applications
8. Bogacz R, Brown E, Mohelis J, Holmes P, Choen JD (2006) The Phyiscs of Optimal Decision MAking: A Formal Analysis of Models of Performance in Two-Alternative Forced-Choice Tasks. Psychol. Rev., 113(4):700-765.
9. Brody C, Romo R, Kepecs A (2003) Basic mechanisms for graded persistent activity: discrete attractors. continuous attractors, and dynamic representations. Curr. Opin. Neurobiol., 13:204-211.
10. Brown E, Holmes P (2001) Modelling a simple choice task: Stochastic dynamics of mutually inihibitory neural growps. Stochastics and Dynamics, 1(2):159-191.
11. Deco G, Martí D (2007) Deterministic Analysis of Stochastic Bifurcations in Multistable Neurodynamical Systems. Biol Cybern 96(5):487-496.
12. Deco G, Scarano L, Soto-Faraco S (2007) Webers Law in Decision Making: Integrating Behavioral Data in Humans with a Neurophysiological Model. The Journal of Neuroscience, 27(42):11192-11200.
13. Evans LC (1998) Partial Differential Equations, AMS.
14. Gardiner CW (1985) Handbook of Stochastic Methods for Physics, Chemistry and the Natural Sciences. Springer-Verlag.

15. Gold JI, Shalden MN (2001) Neural computations that underline decisions about sensory stimuli. TRENDS Cogn. Sci., 5(1):10-16.
16. Gold JI, Shalden MN (2007) The Neural Basis of Decision-Making. Annu. Rev. Neurosci., 30:535-574.
17. La Camera G, Rauch A, Luescher H, Senn W, Fusi S (2004) Minimal models of adapted neuronal response to In Vivo-Like input currents. Neural Computation, 16(10):2101-2124.
18. Michel P, Mischler S, Perthame B (2004) General entropy equations for structured population models and scattering. C.R. Acad. Sc. Paris, Ser. I 338(9):697-702.
19. Michel P, Mischler S, Perthame B (2005) General relative entropy inequality: an illustration on growth models. J.Math.Pures Appl., 84(9):1235-1260.
20. Moreno-Bote R, Rinzel J, Rubin N (2007) Noise-Induced Alternations in an Attractor Network Model of Perceptual Bistability. J. Neurophysiol., 98:1125-1139.
21. Renart A, Brunel N, Wang X (2003) Computational Neuroscience: A Comprehensive Approach. Chapman and Hall, Boca Raton.
22. Rodriguez R, Tuckwell HC (1996) Statistical properties of stochastic nonlinear dynamical models of single neurons and neural networks. Phys. Rev. E, 54:5585-5590.
23. Romo R, Salinas E (2003) Flutter discrimination: neural codes,perception, memory and decision making. Nat. Rev. Neurosci., 4:203-218.
24. Usher, Mc Clelland (2001) The Time Course of Perceptual Choice: The Leaky, Competing Accumulator Model. Phys. Rev., 108(3):550-592.
25. Wilson HR, Cowan JD (1972) Excitatory and inhibitory interactions in localized populations of model neurons. Biophy. J., Vol. 12(1):1-24.
26. Wolka J (1987) Partial Differential Equations. Cambridge University Press.
27. Zhang J, Bogacz R, Holmes P (2009) A comparison of bounded diffusion models for choice in time controlled tasks. J Math. Psychol., 53:231-241.